Grabmayr, P. et al. (1993) Photoabsorption and correlated nucleon pairs. In: 8th Miniconference on Correlations in Hadronic Systems, 9-10 Dec 1993, Amsterdam, The Netherlands.

PHOTOABSORPTION AND CORRELATED NUCLEON PAIRS

P. Grabmayr, T. Hehl, T. Lamparter, J. Leypoldt, A. Mondry, M. Sauer, R. Schneider, K. Spaeth, G.J. Wagner
Physikalisches Institut der Universität Tübingen, D-72076 Tübingen, GERMANY

J.R.M. Annand, P.D. Harty, D.J. MacGregor, J.C. McGeorge, R.O. Owens
Department of Physics and Astronomy, University of Glasgow, U.K.

D. Branford, J. MacKenzie, M. Liang
Physics Department, Edinburgh University, U.K.

A2 collaboration at MAMI, Inst. für Kernphysik, Universität Mainz, GERMANY

Abstract: (γ,2N) and (γ,πN) experiments have been performed on several nuclei using a large area detector setup at the tagged photon facility at MAMI. First results for ^{6}Li are compared with the calibration data from a CD_2 target. The various mechanisms leading to NN final state are discussed. For the $^6Li(\gamma,pn)^4He_{g.s.}$ transition a good description by the Quasi–Deuteron Model was found using 3 body cluster wave functions.

Introduction

From (e,e'p) studies it is known, that the occupancy of shell model orbitals at the Fermi surface is ≈ 80 %, which was attributed to NN correlations [1]. However, no detailed information about their nature can be extracted. Amongst others, one approach to correlations might be the study of (γ,2N) reactions. In particular, the availability of new high precision c.w. electron machines with tagged photon facilities revived the experimental and theoretical efforts for such investigations. However, the knowledge of the various reaction mechanism contributing to the (γ,2N) processes is an essential prerequisite for a detailed discussion of correlations.

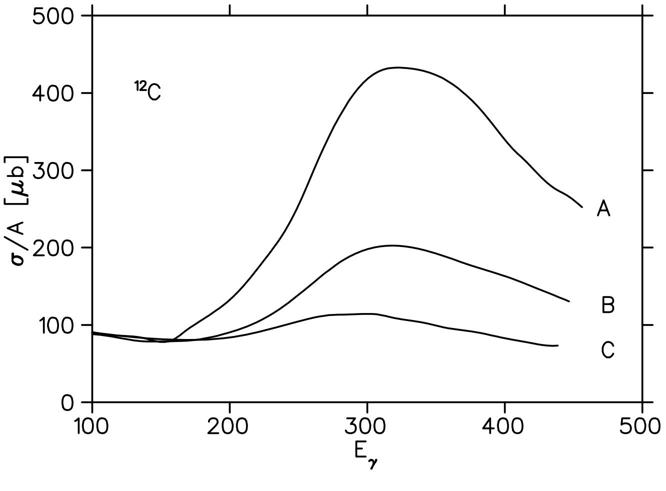

Fig. 1: Total photoabsorption cross sections for ^{12}C (from [3]).

C: genuine two nucleon absorption,
B: two nucleon emission including FSI,
A: total photoabsorption cross section including quasi free π production

The absorption of photons on charged meson exchange currents dominates in the photon energy region ≈ 100 MeV; the two body contributions (genuine 2N absorption) arise both from the "seagull" and the "pion in flight" term [2]. Therefore, the emission of pn pairs is preferred over the T=1 pairs. For higher photon energies (around 300 MeV) Δ-isobar excitations contribute increasingly.

Meanwhile it was realized that back-to-back emitted nucleon pairs can also contribute to the (γ,2N) cross section. Following a one-body photoabsorption the photo pion can undergo final state interaction (FSI) and knock out a nucleon pair. Calculations by Carrasco and Oset [3] showed, that the reabsorption process of real pions increases with the size of the nucleus and shows a maximum at Δ resonance energy. Fig. 1 illustrates this for ^{12}C, where only $\approx 2/3$ of the (γ,2N) cross section (curve B) can be attributed to genuine two body absorption processes (curve C).

Energy and mass dependencies as well as angular correlations of the (γ,2N) and (γ,πN) cross sections will help to disentangle the competing absorption mechanisms. The role of processes with three and more emitted nucleons are predicted by [3]. With a large acceptance detector setup we will detect a significant fraction of multiparticle emissions.

Experiment

To this aim, the (γ,2N) and ($\gamma,\pi N$) reactions have been measured with several targets and over a wide range of photon energies.

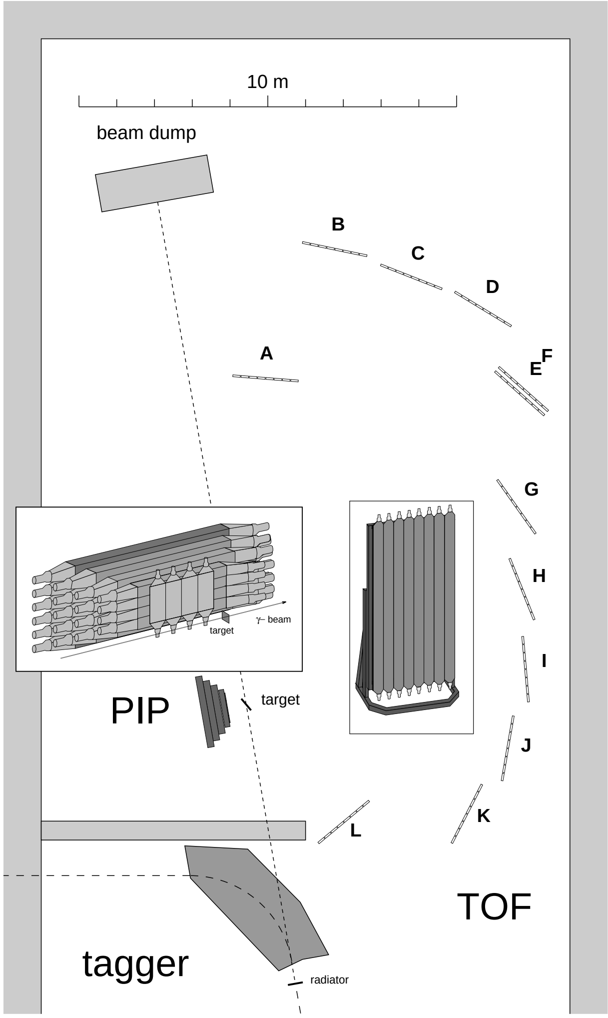

Fig. 2: Detector setup at MAMI.

tagger:	Glasgow photon tagger
PiP:	Pion-Proton hodoscope (left inset)
TOF:	Time-Of-Flight detector array (right inset)

The measurements have been performed at the Mainz Microtron (MAMI), which provides a cw electron beam of 855 MeV. The bremsstrahlung from a 4 μm Ni foil is analyzed by the Glasgow Tagger in the range from 50 to 800 MeV with a bin width of 2 MeV. The target located $\approx$ 7 m downstream from the radiator is surrounded by thin (2 mm) ΔE plastic detectors for particle identification.

For the detection of charged particles (mainly pions and protons), a large acceptance (1 sr) plastic scintillator hodoscope ”PiP” has been employed (Fig. 2, left inset). On the opposite side of the beam, emission angles between 8° and 155° are covered by a 58 m^2 neutron detector system, which consists of 96 vertical plastic scintillator bars ($300\times20\times5$ cm^3 each) and employs the time–of–flight method. With distances varying from 4 to 12 m, a solid angle of 1.2 sr is subtended. Neutrons, protons and pions as well as deuterons and tritons could be identified in TOF with the help of the ΔE detectors. At present the energy resolution of PIP is about 3 MeV for 60 MeV protons, whereas the time resolution of the TOF detector is better than 500 ps. The measured overall missing energy resolution is 6 – 9 MeV.

Preliminary Results

Initial (γ,2N) experiments have been performed on ^{6}Li and ^{12}C. Even without all the necessary corrections, e.g. for position dependencies, the potential of the apparatus can be demonstrated: The missing energy spectrum of CD_2 (Fig. 3) exhibits two peaks. They are interpreted as breakup of the D ($E_m \approx 2$ MeV) and 2N emission from ^{12}C, which has a Q–value of 27 MeV. The breakup of the deuterium results in a two body final state, therefore the width of the first peak (about 6 MeV) is a measure of the energy resolution of the detector system.

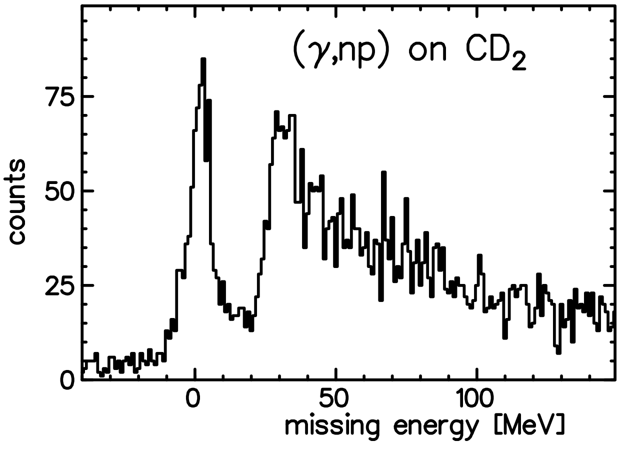

Fig. 3: Missing energy spectrum of $CD_2(\gamma,pn)$.

In Fig. 4, the missing energy spectra for ^{6}Li(γ,pn) and (γ,pp) are shown. ^{6}Li can be described as an α–d–cluster. In this model, the ground state transition ($E_m = +3.7$ MeV) results from breakup of the d cluster. In this case, both nucleons are emitted from the p shell, i.e. from the d–cluster, and the α remains in the ground state. The breakup of the α–core requires more energy, np pairs emitted from (1s1p) and $(1s)^{-2}$ will contribute to the right peak. In contrast, for the emission of proton pairs at least one p has to be knocked out from s shell, thus the respective threshold amounts to $\approx$ 27 MeV.

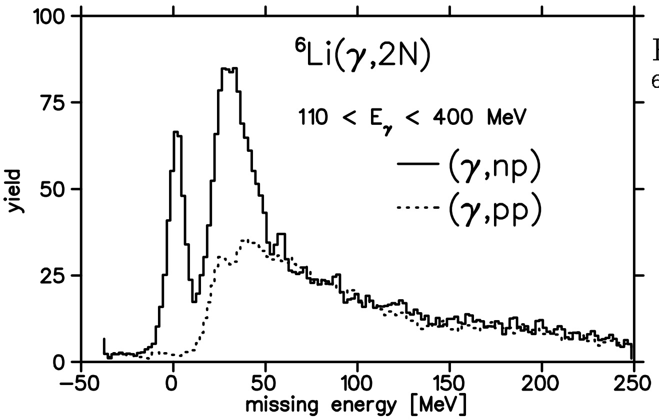

Fig. 4: Missing energy spectra of ^{6}Li(γ,pn) and (γ,pp).

The long tail for $E_m > 60$ MeV has similar shapes for both the (γ,pn) and (γ,pp) channel. For demonstration, the (γ,pp) has been normalized accordingly. The strengths at larger missing energies are attributed to contributions from multinucleon emission or FSI.

For the investigation of ground state properties (i.e. $-5 < E_m < 10$ MeV), we plot the excitation function in the range $110 < E_\gamma < 400$ MeV. Here, the (γ,pn) process is expected to be comparable to the breakup of the D. Indeed, as Fig. 5 shows the two yield curves are very similar. The analysis showed, that the γ, n and p are coplanar; which suggests, that only these two particles have been emitted. MECs contribute mostly to (γ,pn); most of the (γ,pp) strength below pion threshold is likely to arise from FSI, whereas for higher E_γ Δ–excitations and multinucleon emissions can result in both (γ,pp) and (γ,pn).

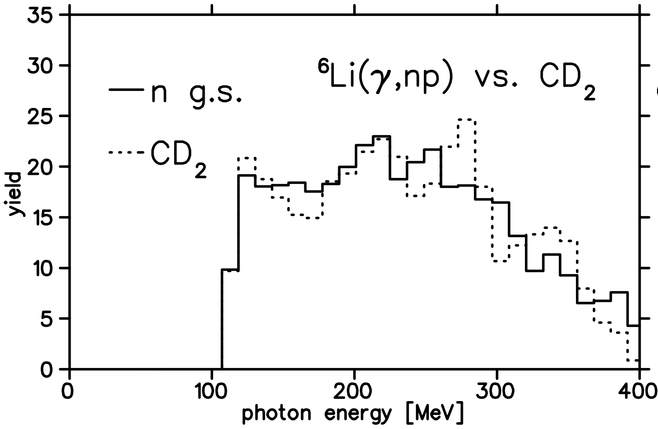

Fig. 5: Excitation functions of ^{6}Li(γ,pn)$_{g.s.}$ and D-breakup of CD$_2$.

In contrast to $(1p)^{-2}$ pairs, emissions of pp and np pairs involving 1s–nucleons show increasing yields for photon energies around Δ–resonance energies (Fig. 6). This can be explained (i) by higher Fermi momenta available in the s shell and (ii) by a higher probability of sequential processes following quasi-free π–production. The small amount of pp pairs from the same missing energy region as selected for the ^{6}Li(γ,pn)^{4}He$_{g.s.}$ transition is probably due to random coincidences in TOF, which have not been subtracted so far. Note, that neutron efficiencies have not been corrected for this plot.

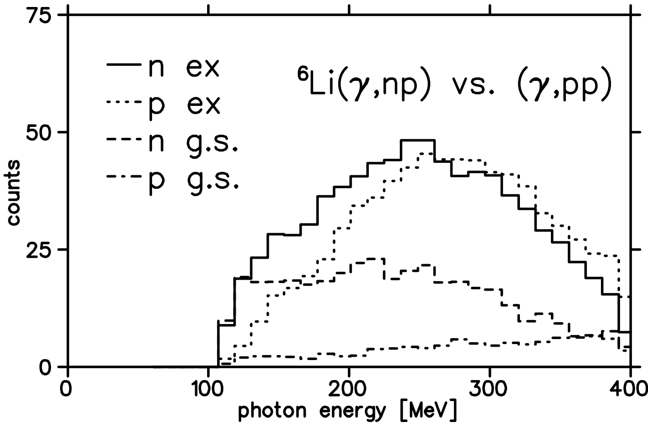

Fig. 6: Comparison of ^{6}Li(γ,pn) and (γ,pp) for g.s. transitions and transitions involving 1s–nucleon involved (20 < E_m < 40 MeV)

Another test of the α–d cluster picture of ^{6}Li is performed by the comparison of measured missing momentum distributions with theoretical predictions. Monte Carlo calculations based on cluster wave functions by Kukulin et al. [5] reproduce the maximum of the ground state momentum distribution at 50 MeV/c very well. To study the (1s1p) and $(1s)^{-2}$ pair emission a missing energy range of 20 < E_m < 40 MeV was selected. The resulting distribution is compared in Fig. 7 right to the ground state transition.

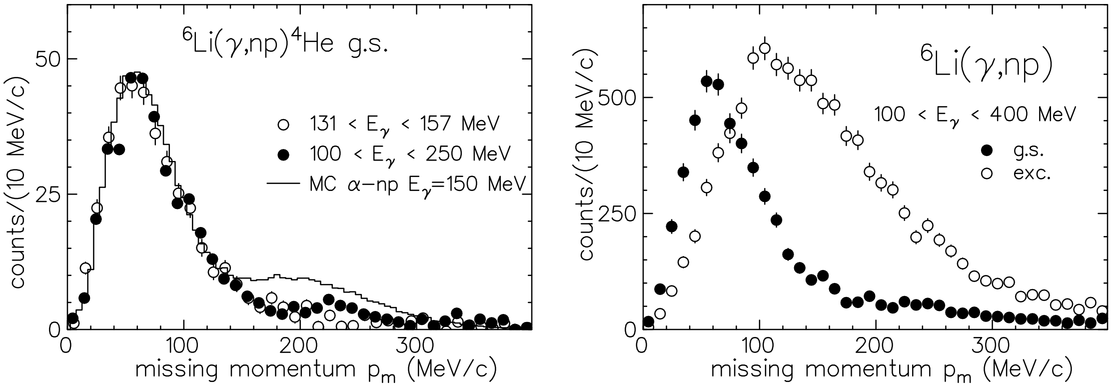

Fig. 7: Missing momentum distributions for ^{6}Li(γ,pn)^{4}He$_{g.s.}$ compared with MC calculations (left part) and excited state (right part).

Conclusions

The nucleus ^{6}Li presents a good case for studies of the Quasi–Deuteron picture of the photoabsorption process. In this case, the cluster model is a good description of the nuclear structure to understand the role of the quasi–deuteron, namely the $(1p)^2$ np pair. We showed, that this picture is well justified for photon energies up to 400 MeV by the similarity of excitation functions of the breakup of the deuteron and the ^{6}Li(γ,pn)^{4}He$_{g.s.}$ transition as well as by a good description of the missing momentum distribution by α–np–cluster wave function. Furthermore, the influence of the Δ–resonance was shown to be important for transitions to excited states. The comparison of (γ,pn) and (γ,pp) will help to identify the contributions due to MECs.

For a detailed theoretical modeling of the reactions, the calculations should include the photoabsorption processes in the nucleus themselves by a microscopic model. Other essential ingredients are assumptions on correlations between nucleons and the inclusion of FSI of nucleons and mesons [4,6].

References

[1] P. Grabmayr, Prog. Part. Nucl. Phys. **29**(1992)221
[2] J. Ryckebusch et al., Phys.Lett. **B291**(1992)213
[3] R.C. Carrasco and E. Oset, Nucl. Phys. **A536**(1992)445
[4] J.Ryckebusch et al., submitted to Nucl. Phys. A
[5] V.I. Kukulin et al., Nucl. Phys.**A513**(1990)221
[6] R.C Carrasco et al., Nucl. Phys. A preprint 1759

This work was supported by the BMFT, EEC, SERC, DAAD, DFG and NATO.